  Bull. Chem. Soc. Jpn., 61, 621—626 (1988)

Catalytic Properties of Perovskite-Type Mixed Oxides (ABO_3) Consisting of Rare Earth and 3d Transition Metals. The Roles of the A- and B-Site Ions

Taihei NITADORI,†,* Tatsumi ICHIKI,†† and Makoto MISONO
Department of Synthetic Chemistry, Faculty of Engineering, The University of Tokyo, Hongo, Bunkyo-ku, Tokyo 113
†Central Research Institute, Japan Tobacco, Inc., Umegaoka, Midori-ku, Yokohama, Kanagawa 227
(Received April 1, 1987)

The catalytic activities of perovskite-type mixed oxides ($LnBO_3$ and $Ln_{0.8}Sr_{0.2}CoO_3$, Ln=rare-earth (lanthanoid) elements, B=3d transition metals) for the oxidation of propane and methanol have been studied comparatively. It has been found that the catalytic activities of $LnBO_3$ were principally determined by the B-site elements and were similar to those of the corresponding oxides of the B-site elements. The roles of the rare-earth ions of the A-site were secondary as long as they were trivalent. Upon the partial replacement of Ln^{3+} by Sr^{2+}, the catalytic activities of $LnCoO_3$ increased several times, the magnitude of the increase being similar among all the rare-earth ions. These results demonstrate that the kind and the valence of a B-site metal are of primary importance for the control of the catalytic activity for oxidation, almost regardless of the kind of trivalent rare-earth elements at the A-site.

Perovskite-type mixed oxides (ABO_3) are typical mixed oxides and many are known with various A- and B-site ions.[1] Because of this nature and the stability of the perovskite structure, the compositions and oxygen vacancies as well as the oxidation state of metal ions can be varied in a regular way. These oxides are, therefore, suitable model compounds for the study of the relationships between the solid state chemistry and the catalytic action of mixed metal oxides. Moreover, the perovskite-type mixed oxides with Co or Mn ions on the B-site have possible applications as fuel cell electrodes[2] and oxidation catalysts.[3,4]

We previously reported some remarkable effects of the valence control of the B-site ions and reasonably explained those effects in terms of the redox properties of the catalysts. For example, the Sr substitution for La of $LaCoO_3$ changed the catalytic activity greatly; paticularly, $La_{0.8}Sr_{0.2}CoO_3$ was the most active, and its activity for oxidation was higher than a Pt catalyst.[4] We further investigated the effects of the Sr, Ce, and Hf substitutions of $LaBO_3$ (B=Co, Fe, and Mn).[5–9] These studies confirmed that the valence of the B-site ions and the oxygen or metal vacancy in the bulk phase are the most important factors controlling the catalytic properties. It was revealed at the same time that the effects of those factors significantly changed with the kind of constituent element.

Therefore, in the present work, in order to elucidate more generally the roles of the constituent elements, we investigated comparatively the effects of rare-earth ions at the A-site and of 3d transition metal ions at the B-site. The effects on the valence control were examined in the case of the Sr substitution for $LnCoO_3$, which previously showed a remarkable positive effect. Although several works on those effects have been reported,[4,10–16] there have been very few studies in which both A- and B-site ions were varied simultaneously and extensively, and no studies about the effect of the A-site ion in valence control.

Experimental

Catalysts. The perovskite-type mixed oxides used as catalysts are summarized in Table 1. They were prepared from mixtures of metal nitrates of each component in the same manner as has been described in the previous paper.[4] The precipitates which had been obtained from mixed nitrate solutions by adding butylamine were filtered, decomposed in air at 300 °C for 3 h, and calcined in air, usually at 850 °C for 5—10 h. Some were calcined at 1100 °C for 10 h. Powder X-ray diffraction patterns were recorded on a powder X-ray diffractometer (Rigaku Denki, Rotaflex, RU-200) using Cu $K\alpha$ radiation. The surface areas of the samples were measured by means of the BET method (N_2 adsorption).

Component single oxides (rare earth=La, Ce, Pr, Nd, Sm, Eu, and Gd; 3d transition metal=Mn, Fe, and Co) were obtained by the calcination of metal acetates or nitrates of a reagent grade at 850 °C for 5 h in air. XPS measurements were carried out for $La_{1-x}Sr_xCoO_3$ with the Mg $K\alpha$ (1253.6 eV) source by the use of ESCA 750 (Shimadzu). The binding energies were calibrated with reference to a Cls electron line (285.0 eV).

Apparatus. Conventional flow, pulse, and closed circulation systems as described before[4–6] were used.

Procedure. Catalytic Oxidation of Propane and Methanol: The oxidation reactions of propane and methanol were carried out with the flow system following the procedure described previously.[4,9] Prior to the reaction, the catalysts (300 mg) were usually pretreated in an O_2 stream for 1 h at 300 °C. A gas mixture of propane (0.83%), O_2 (33.3%), and N_2 (balance) was used for the propane oxidation, and a mixture of methanol (6.0%), O_2 (9.0%), and N_2 (balance) for the methanol oxidation.

Reduction of Catalysts by CO: The reduction of catalysts by CO was carried out with the circulation system. Before the reduction, the catalysts (300 mg) were treated in

†† Present address: Tonen Sekiyukagaku K. K., Ohimachi, Saitama.

O_2 at 300 °C for 1 h, and then they were evacuated for 1 h at the reduction temperature. The initial CO pressure was about 20 Torr (1 Torr=133.3 Pa). The rates of the reduction were measured by the pressure decrease of CO, while the CO_2 produced was condensed in a trap kept at the temperature of liquid nitrogen.

Temperature-Programmed Desorption (TPD) of Oxygen: The TPD of oxygen was carried out using helium as a carrier gas (25 cm^3 min^{-1}) as has been described previously.[9] Prior to each run, the sample (1 g) was pretreated in an O_2 stream at 300 °C for 1 h (except for the $LnMnO_3$'s, which were pretreated at 800 °C). The rate of the temperature rise was 20 deg min^{-1}. In the first run for each sample, CO_2 and H_2O envolved in addition to O_2. In the subsequent runs, however, neither CO_2 nor H_2O was detected above the background level, and the TPD curves were reproducible. The data of the second runs were, therefore, adopted as in the previous papers.[5,9]

Results

Structures and Surface Areas of Perovskite Catalysts. The surface areas and the crystal structures of the catalysts used in the present study are summarized in Table 1. Perovskite-type structures of the samples were confirmed by reference to ASTM cards. The XRD patterns of these samples showed only the perovskite structure. The diffraction peaks of $LaFeO_3$ and $GdFeO_3$ calcined at 1100 °C became narrower, and the surface areas smaller, indicating the increased crystallinity. According to XRD, all of the rare-earth oxides were sesqui-oxides except for CeO_2 and Pr_6O_{11}; the oxides of the component 3d transition metals prepared were Mn_2O_3, Fe_2O_3, and Co_3O_4.

Table 1. Surface Area and Structure of Catalysts

Catalyst	Calcination		Surface area/m^2g^{-1}	Structure[a]
	Temp/°C	Time/h		
$LaCoO_3$	850	10	1.8	P(R)
$PrCoO_3$	850	10	2.1	P(C)
$NdCoO_3$	850	10	2.2	P(C)
$SmCoO_3$	850	10	2.4	P(O)
$EuCoO_3$	850	10	1.0	P(O)
$GdCoO_3$	850	10	2.0	P(O)
$LaFeO_3$	850	5	6.8	P(O)
	1100	10	0.4	P(O)
$SmFeO_3$	850	5	4.9	P(O)
$GdFeO_3$	850	5	5.2	P(O)
	1100	10	0.4	P(O)
$LaMnO_3$	850	10	8.3	P(O)
$SmMnO_3$	850	10	7.3	P(O)
$GdMnO_3$	850	10	6.8	P(O)
$La_{0.8}Sr_{0.2}CoO_3$	850	10	3.0	P(C)
$Pr_{0.8}Sr_{0.2}CoO_3$	850	10	2.2	P(C)
$Nd_{0.8}Sr_{0.2}CoO_3$	850	10	2.9	P(C)
$Sm_{0.8}Sr_{0.2}CoO_3$	850	10	4.6	P(O)
$Eu_{0.8}Sr_{0.2}CoO_3$	850	10	3.6	P(O)
$Gd_{0.9}Sr_{0.1}CoO_3$	850	10	3.8	P(O)
$Gd_{0.8}Sr_{0.2}CoO_3$	850	10	5.5	P(O)
$Gd_{0.6}Sr_{0.4}CoO_3$	850	10	3.4	P(O)

a) P: perovskite structure, R: rhombohedral, C: cubic O: orthorhombic (judged from the splitting of the main peaks).

The surface composition of $La_{1-x}Sr_xCoO_3$, as estimated by XPS, is shown in Table 2. It was calculated from Eq. 1.[17]

$$\frac{N_a}{N_b} = \frac{n_a \cdot \lambda_a \cdot \sigma_a \cdot s_a}{n_b \cdot \lambda_b \cdot \sigma_b \cdot s_b} \quad (1)$$

where N: peak intensity, n: atoms per unit volume, λ: mean free path of electron, σ: ionization cross-section, and s: instrumental factor. The peak areas of La4d, Co2p (the average of 2p3/2 and 2p1/2) and Sr3d, including the satellite peak, were used for N, while the values of σ were taken from the literature.[18] "$\lambda \cdot s$" was assumed in this study to be constant, as has been suggested by the manufacturer. This assumption is not very accurate (though the errors are estimated to be no more than 15%), but it may be sufficient to compare the relative change in the surface composition for a series of catalysts. Therefore, the data in Table 2 may be considered as semi-quantitative values reflecting the trends of the surface segregation compared with the bulk composition. Thus, it may be stated, on the basis of the data in Table 2, that La was richer on the surface than in the bulk and that the Co content increased monotonically with an increase in the Sr content. The binding energies (780.3—780.9 and 795.5—796.1 eV), the spin-orbit splitting (15.2 eV), and the satellite splitting (9.8—10.0 eV) for Co2p were consistent with those of Co^{3+}.[19] Therefore, most of the Co in the surface may be Co^{3+}, although the possibility of the presence of Co^{4+} can not be excluded, since no data were reported for Co^{4+}.

Comparison of the Catalytic Activity for Oxidation. The catalytic activities of the perovskites and the rare-earth oxides for propane oxidation are shown in Fig. 1A, where are given the rates normalized to the unit surface area. CO_2 and H_2O were the only products in these experiments. It is notable that the Ln ions at A-site had a much smaller effect on the activity than did the transition metal ions at B-site, the order of the activity being always $LnCoO_3 > LnMnO_3 \gg LnFeO_3$. The activities of the component rare-earth oxides were very low. The activation energies obtained from the data at low conversion levels in these

Table 2. The Surface Compositions of $La_{1-x}Sr_xCoO_3$

	$x=0$		$x=0.2$			$x=0.6$		
	La	Co	La	Sr	Co	La	Sr	Co
Surface	0.68	0.32	0.48	0.14	0.38	0.26	0.23	0.51
Bulk[a]	0.50	0.50	0.40	0.10	0.50	0.20	0.30	0.50

a) Calculated from the starting materials.

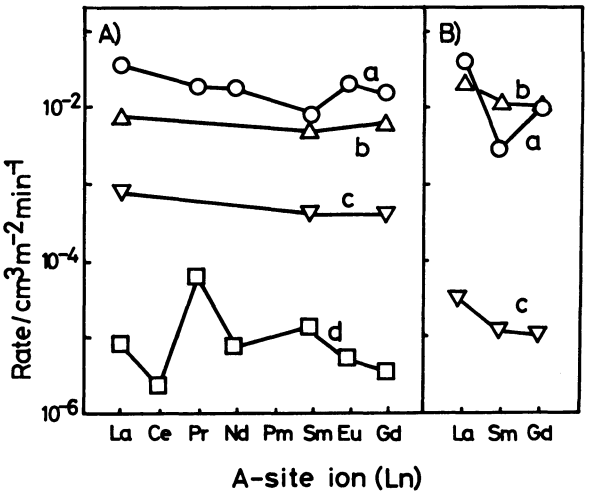

Fig. 1. Catalytic activities of perovskites and rare-earth oxides for propane oxidation at 227 °C and methanol oxidation 200 °C.
a: $LnCoO_3$, b: $LnMnO_3$, c: $LnFeO_3$, d: Ln oxide.
A) Propane, B) methanol.

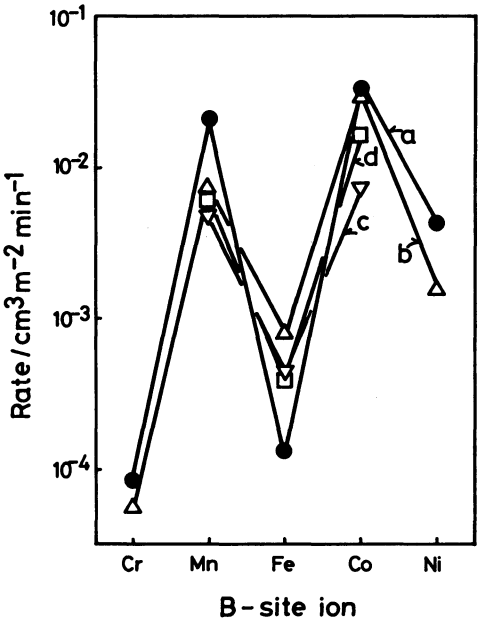

Fig. 2. Catalytic activities of perovskite and B-site oxide for propane oxidation at 227 °C.
a: Oxides of B-site metals, b: $LaBO_3$, c: $SmBO_3$, d: $GdBO_3$.

experiments were 18.2—20.9 kcal mol^{-1} ($LnCoO_3$), 19.5—21.6 ($LnMnO_3$), and 24.0—25.8 ($LnFeO_3$), respectively. The greater effect of B-site ions than of Ln ions was also observed for methanol oxidation, as is shown in Fig. 1B (Co, Mn≫Fe). Complete oxidation was again the only reaction observed. The activation energies were 47—55 kcal mol^{-1}. The methanol oxidation was also measured over $LaFeO_3$ and $GdFeO_3$, which had been calcined at 1100 °C. In

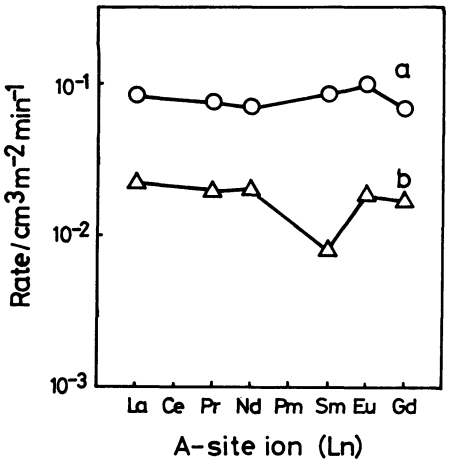

Fig. 3. Catalytic activities of $Ln_{0.8}Sr_{0.2}CoO_3$ for propane oxidation at 227 °C.
a: $Ln_{0.8}Sr_{0.2}CoO_3$, b: $LnCoO_3$.

this case also, the difference in Ln had only a small effect.

The activity patterns of the perovskites and metal oxides containing the same 3d metals are compared in Fig. 2, including those of Cr[20] and Ni.[4] The differences in the activities among the catalysts on the whole were more than two orders of magnitude, whereas the differences between the perovskites and the corresponding B-site oxide were less than one order; also both the perovskites and B-site oxides showed very similar activity patterns, with twin peaks at Mn and Co. A similar pattern has been reported for $LaBO_3$ by Tascon et al.[21] This pattern resembles the trend reported for the oxidation of CH_4 and H_2[22] and may, therefore, be considered to reflect the ability of metal oxide to activate O_2. This pattern is different from the so called "Dowden pattern."[23] The Dowden pattern, which was often observed for hydrogenation reactions and which reflects the ability to activate H_2, has twin peaks at Cr and Co.

The Effect of Sr Substitution at A-Site for the Catalytic Activity. The effect of Sr substitution was examined for several rare-earth ions in the case of $LnCoO_3$, since a marked increase in the catalytic activity was previously found for $LaCoO_3$.[5,6] As shown in Fig. 3, the substitution by Sr for 20% of the A-site ions of $LnCoO_3$ increased 5—10 times the catalytic activity for propane oxidation; the magnitude of the increase was similar among the rare-earth ions. The surface areas tended to increase upon the Sr substitution, so the increases in the catalytic activity per catalyst weight were still greater. Figure 4 shows the effect of the extent of Sr substitution for $GdCoO_3$, together with the previous results for $LaCoO_3$.[4-6] The oxidation activity varied similarly for both systems, showing maxima at x=0.1—0.2. A similar effect was also found for methanol oxidation.

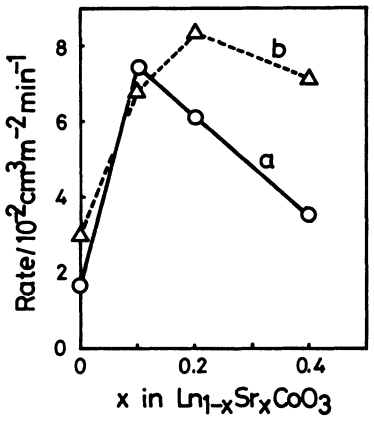

Fig. 4. Effect of Sr substitution on the catalytic activities of $LnCoO_3$ for oxidation of propane at 227 °C.
a: $Gd_{1-x}Sr_xCoO_3$, b: $La_{1-x}Sr_xCoO_3$.

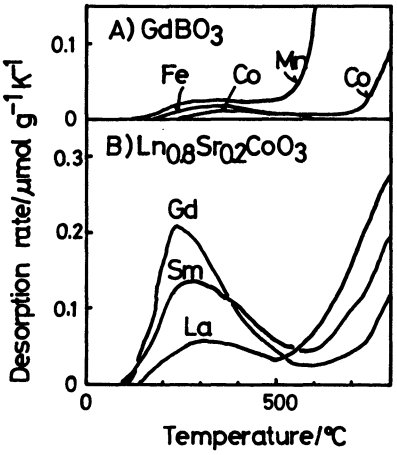

Fig. 5. TPD profiles of oxygen from perovskites.
A) $GdBO_3$, B) $Ln_{0.8}Sr_{0.2}CoO_3$.

TPD of Oxygen. Figure 5A shows the TPD of oxygen from $GdBO_3$ (B=Co, Fe, and Mn). Each TPD curve resembles that we previously reported for $LaBO_3$, with the same B-site element.[5,7,9] Broad and low peaks appeared at 150—500 °C for all three samples. The amounts of oxygen desorbed below 500 °C, which were previously indicated to be related to the catalytic function, were small, the order being Mn>Fe>Co. Even for $GdMnO_3$ the amount was only 0.12 cm^3 g^{-1}, which corresponded to 0.3 times the surface monolayer of oxygen. The large peak for Mn above 500 °C is likely to be due to the removal of excess oxygen, as has been discussed previously for $LaMnO_3$.[9]

The TPD profiles of $Ln_{0.8}Sr_{0.2}CoO_3$ (Ln=La, Sm, and Gd) are shown in Fig. 5B. The amounts of oxygen desorbed increased remarkably upon the Sr substitution, as has previously been reported for the $LaCoO_3$ system.[5,24] The amounts of oxygen desorbed

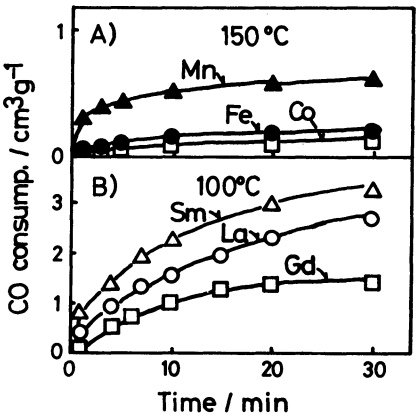

Fig. 6. Reduction of perovskite by CO.
A) $GdBO_3$, B) $Ln_{0.8}Sr_{0.2}CoO_3$.

below 500 °C were 0.34 (La)<0.82 (Sm)<1.00 (Gd) cm^3 g^{-1}. These values corresponded to about 0.6 (La) and 1.0 (Sm, Gd) surface monolayer. The amounts desorbed up to 800 °C were 1.17 (La), 1.40 (Sm), and 1.31 (Gd) cm^3 g^{-1}, which corresponded to 1.3—2.2 surface monolayers. Since the adsorbed oxygen is usually scarce, significant parts of the desorbed oxygen are from the catalyst bulk.

Reduction of the Catalyst by CO. Figure 6A shows the rate of the CO consumption of $GdBO_3$ (B=Co, Fe, and Mn) as measured in the circulation system at 150 °C. The amounts of CO consumed in 30 min were 0.1 (Co), 0.21 (Fe), and 0.63 (Mn) cm^3 g^{-1}, respectively, values which corresponded to 0.1—0.4 surface monolayer of oxygen. This tendency agreed with that of the amount of oxygen desorbed below 500 °C in the TPD described above (Fig. 5A). Figure 6B shows the results of the reduction for $Ln_{0.8}Sr_{0.2}CoO_3$ at 100 °C. $Ln_{0.8}Sr_{0.2}CoO_3$ was appreciably more easily reduced by CO than by $LnBO_3$ in spite of the lower reduction temperature. The amounts of CO consumed in 30 min were 2.27 (La), 3.35 (Sm), and 1.42 (Gd) cm^3 g^{-1}, corresponding to 2.6, 2.0, and 0.7 surface monolayers, respectively.

Discussion

Roles of A- and B-Site Ions. We have previously reported that the catalytic activities of $LaBO_3$ (B=Fe, Co, and Mn) for the oxidations of hydrocarbons and CO were approximately on the same level at those of the oxides of the B-site metals and that the catalytic properties reflected mainly the nature of the B-site metals.[4] This has also been pointed out by other investigators.[10-14] To explain this, the electronic state of the d electron of the B-site ion,[11] the binding energy of the B–O bond,[12] and the stabilization energy of the crystal field[13] have been proposed as the controlling factors of the catalytic activity. Although these factors are different, all of these explanations are based on the

nature of the B-site ions.

In this study, the rare-earth ion (Ln) at the A-site was changed variously. It was thus found that the effect of Ln was relatively small (Fig. 1) and that the activity patterns of the peroviske catalysts were the same as that of the oxides of the B-site transition metals (Fig. 2). By contrast, the order of the catalytic activities observed for the rare-earth oxides was quite different from that of the corresponding perovskites, and the activities were much lower. Among them, Pr_6O_{11} was the most active, and CeO_2, the least. This tendency is in agreement with the result reported for butane oxidation by Hattori et al.,[25] while it is different from the trend for $LnCoO_3$.

The physical properties of the rare-earth ions, such as the ionic radius, the charge density, and the magnetic moment, change significantly from La to Gd. The structures of the perovskites containing these elements also vary, for example, from $LaCoO_3$ (rhombohedral) to $GdCoO_3$ (orthorhombic). These changes would influence the electronic state of the B-site ion, but the effect seems less important than the B-site element itself. Thus, the effect of the A-site ion is presumed to be secondary as long as it is trivalent.

Nevertheless, several examples in which this secondary effect is significant have been reported. Parkash et al.[15] observed the highest activities for CO oxidation for Nd and Ho among $LnCoO_3$ (Ln=La, Pr, Nd, Gd, and Ho) and discussed this result based on the relative ratio of low- to high-spin Co^{3+}. Arakawa et al. reported that the catalytic activity of $LnFeO_3$ (calcined at 1200 °C) for methanol oxidation increased remarkably from La to Gd; they concluded that this was a result of the decrease in the covalency of the Fe–O bond.[16] In the present study, the catalytic activity for methanol oxidation over $LnFeO_3$ did not change much (Fig. 1B). Though the reason for this difference is not clear at present, the alteration of the composition on the surface and/or in the bulk of the catalyst might have occurred because of the different calcination conditions.

The Effects of Ln for the Valance Control of $LnCoO_3$. The catalytic activity increased several times upon the Sr substitution for Ln of $LnCoO_3$ regardless of the kind of trivalent rare-earth ion (Fig. 3). As for the extent of the substitution, a maximum was observed at x=0.1 for $Gd_{1-x}Sr_xCoO_3$ (Fig. 4). These results generally agree with our previous results for $La_{1-x}Sr_xCoO_3$.[6] The catalytic activity of $La_{1-x}Sr_xCoO_3$ increased initially with an increase in x and showed a maximum at x=0.2. This variation in activity was semi-quantitatively explained as follows based on the change in the oxidation-reduction properties of the catalyst.[5,6]

Upon the Sr substitution, a part of the Co^{3+} is oxidized to Co^{4+} (Eq. 2). Since the Co^{4+} is unstable, however, the oxide ions tend to be removed and the Co^{4+} returns to Co^{3+} (Eq. 3):[5,6,24,26]

$$Ln^{3+}Co^{3+}O_3 \xrightarrow{Sr} Ln^{3+}_{1-x}Sr^{2+}_xCo^{3+}_{1-x}Co^{4+}_xO_3 \quad (2)$$

$$Ln_{1-x}Sr_xCo^{3+}_{1-x}Co^{4+}_xO_3 \longrightarrow Ln_{1-x}Sr_xCo^{3+}_{1-x+2\delta}Co^{4+}_{x-2\delta}O_{3-\delta} + (\delta/2)O_2 \quad (3)$$

This is in agreement with the present results that the oxygen desorbed in TPD increased remarkably and that the reduction by CO became much easier upon the Sr substitution (Figs. 5 and 6). This means that the oxidation power of $LnCoO_3$ is increased by the valence control. Since the increase in the oxidation power promotes the catalytic activity of the oxide catalysts for oxidation, the initial increase in the activity by the Sr substitution is understandable. The decrease in the catalytic activity at higher extents of substitution may be explained by the slower re-oxidation step in the redox cycle of the catalysts, as has been demonstrated previously,[6] or by the lower reactivity of the surface oxygen.[27] Therefore, the mechanism of the Sr substitution for $LnCoO_3$ in the valence control and the catalytic activity may be similar to that for $LaCoO_3$. The possibility that an unknown La- or Sr-rich phase segregated on the surface of the perovskites having high Sr contents and lowered the activity may not be excluded. However, this is not likely to be the main reason for the decrease in activity, since the surface compositions estimated by XPS indicated monotonous changes in the Co and Sr contents when x was increased (Table 2).

There were relatively small, but definite, differences between $LnCoO_3$'s, and the trends among the Ln ions observed for the TPD, the reducibility and the catalytic activity did not agree well with one another. For example, the amount of oxygen desorbed in TPD for $Ln_{0.8}Sr_{0.2}CoO_3$ (Fig. 6B; Gd>Sm>La for 25—500 °C) did not parallel the catalytic activity (Fig. 3; La>Gd>Sm) and the reducibility of $Ln_{0.8}Sr_{0.2}CoO_3$ (Fig. 6B; Sm>La>Gd). The reason for the disagreement observed for the secondary effects is not clear at present. Part of these discrepancies may, however, be related to the difference in the compositions between the surface and bulk or to the differences in the relative rates of the chemical processes on the surface to those in the bulk. A possible example of the chemical processes is the supply of oxygen species to surface sites. It can be from the gas phase through adsorption or from the bulk through diffusion.

The effect of Sr substitution on the Mn systems was examined only for $La_{1-x}Sr_xMnO_3$,[9] but the effects may be similar for other Ln ions, because it was reported by Raj et al.[28] that $LnMnO_3$ (Ln: La—Gd) calcined in air 950 °C has a similar oxidative nonstoichiometry. As the Sr content increases, the composition changes from oxygen-excess to oxygen-deficient and the catalytic activity changes moderately, showing maxima at about x=0.6.[9]

Conclusion

The following conclusions may be deduced for the roles of the A- and B-site ions of $LnBO_3$ for oxidation catalysis: (i) the kind and valence of the 3d transition metal ion at the B-site are of primary importance, (ii) the role of the rare-earth ion at the A-site is secondary as long as it is trivalent, (iii) the substitution of the A-site ion by ions with a different valence is very influential; this is caused by the change in the oxidation state of the B-site ion and the formation of an anion vacancy.[4-9]

References

1) R. J. H. Voorhoeve, "Advanced Materials in Catalysis," ed by J. J. Burton and R. L. Garten, Academic Press, New York (1977), p. 129.
2) D. B. Meadowcroft, *Nature (London)*, **226**, 847 (1970).
3) W. F. Libby, *Science*, **171**, 499 (1971).
4) T. Nakamura, M. Misono, T. Uchijima, and Y. Yoneda, *Nippon Kagaku Kaishi*, **1980**, 1679.
5) T. Nakamura, M. Misono, and Y. Yoneda, *Bull. Chem. Soc. Jpn.*, **55**, 394 (1982); *Chem. Lett.*, **1981**, 1585.
6) T. Nakamura, M. Misono, and Y. Yoneda, *J. Catal.*, **83**, 151 (1983).
7) T. Nitadori and M. Misono, *J. Catal.*, **93**, 459 (1985).
8) M. Misono and T. Nitadori, "Adsorption and Catalysis on Oxide Surface," Elsevier, Amsterdam (1985), p. 409.
9) T. Nitadori, S. Kurihara, and M. Misono, *J. Catal.*, **98**, 221 (1986).
10) N. Yamazoe and Y. Teraoka, *Shokubai*, **25**, 196 (1983).
11) R. J. H. Voorhoeve, J. P. Remeika, and L. E. Trimble, *Ann. N. Y. Acad. Sci.*, **272**, 3 (1976).
12) T. Shimizu, *Chem. Lett.*, **1980**, 1.
13) J. M. D. Tascon and L. G. Tejuca, *React. Kinet. Catal. Lett.*, **15**, 185 (1980).
14) W. B. Li, H. Yoneyama, and H. Tamura, *Nippon Kagaku Kaishi*, **1982**, 761.
15) O. Parkash, P. Ganguly, G. R. Rao, C. N. R. Rao, D. S. Rajoria, and V. G. Hide, *Mater. Res. Bull.*, **9**, 1173 (1974).
16) T. Arakawa, S. Tsuchiya, and J. Shiokawa, *J. Catal.*, **74**, 317 (1982).
17) K. Hirokawa, *Hyomen Kagaku*, **7**, 237 (1986).
18) J. H. Scofield, *J. Electr. Spectr. Relat. Phenom.*, **8**, 129 (1976).
19) J. Okamoto, H. Nakano, T. Imanaka, and S. Teranishi, *Bull. Chem. Soc. Jpn.*, **48**, 1163 (1975).
20) T. Nitadori and M. Misono, unpublished data.
21) G. Kremenic, J. M. L. Nieto, J. M. D. Tascon, and L. G. Tejuca, *J. Chem. Soc., Faraday Trans. 1*, **81**, 939 (1985).
22) G. K. Boreskov, *Kinet. Katal.*, **14**, 2 (1973).
23) D. A. Dowden, *Catal. Rev. Sci. Eng.*, **5**, 1 (1972).
24) N. Yamazoe, Y. Teraoka, and T. Seiyama, *Chem. Lett.*, **1981**, 1767.
25) T. Hattori, J. Inoko, and Y. Murakami, *J. Catal.*, **42**, 60 (1976).
26) H. Obayashi, T. Kudo, and T. Gejo, *Jpn. J. Appl. Phys.*, **13**, 1 (1974).
27) Y. Teraoka, M. Yoshimatsu, N. Yamazoe, and T. Seiyama, *Shokubai*, **26**, 106 (1984).
28) S. Louis Raj and V. Srinivasan, *J. Catal.*, **65**, 121 (1980).